

# Directionally solidified microstructures and peritectic phase growth of Cu-75%Sn peritectic alloy<sup>①</sup>

LI Shuang-ming(李双明)<sup>1</sup>, LÜ Haiyan(吕海燕)<sup>1</sup>, ZHANG Rong(张蓉)<sup>2</sup>,  
LIU Lin(刘林)<sup>1</sup>, FU Heng-zhi(傅恒志)<sup>1</sup>

(1. State Key Laboratory of Solidification Processing,  
Northwestern Polytechnical University, Xi'an 710072, China;

2. Department of Applied Physics,  
Northwestern Polytechnical University, Xi'an 710072, China)

**Abstract:** Directionally solidified microstructures of Cu-75%Sn peritectic alloy were investigated at the growth rate ranging from 1 to 300  $\mu\text{m/s}$ . With the growth rate increasing, directionally solidified plate-like microstructures in Cu-75%Sn peritectic alloy are refined by the increase of nucleation quantities of primary  $\epsilon$  phases and cooling rate. Peritectic  $\eta$  phase can grow by the peritectic transformation and direct solidification from the liquid. At the low growth rate varying from 5 to 10  $\mu\text{m/s}$ , the width of  $\epsilon$  phase increases due to the effect of the peritectic transformation; however, at higher growth rate, the deviation between the width of  $\epsilon$  phase and the whole plate-like microstructure increases resulting from direct solidification of  $\eta$  phase from the undercooled melt. The regressed data show that the relationship between the width of the whole plate-like microstructure ( $W$ ) and the growth rate ( $v$ ) satisfies as  $Wv^{0.27} = 117 \mu\text{m}^{1.27} \cdot \text{s}^{-0.27}$  and the primary dendritic arm spacing ( $\lambda$ ) with the growth rate has a relation of  $\lambda^{0.208} = 153.8 \mu\text{m}^{1.208} \cdot \text{s}^{-0.208}$  as the growth rate increases from 3 to 300  $\mu\text{m/s}$ .

**Key words:** Cu-75%Sn alloy; peritectic alloy; directional solidification; primary dendritic arm spacing

**CLC number:** TG 132.32

**Document code:** A

## 1 INTRODUCTION

Peritectic reaction is the formation of peritectic phase by reaction of the primary precipitation solid phase directly with the liquid at peritectic temperature, clearly different from the solidification aspects of single phase and eutectic system. Recently, many technically important materials, including high-temperature structural materials, Ti-Al and Ni-Al alloys<sup>[1, 2]</sup>, stainless steel Fe-Cr-Ni alloy<sup>[3]</sup> and permanent magnetic materials, Nd-Fe-B and Sm-Co-Cu alloys<sup>[4, 5]</sup>, are manufactured by the peritectic solidification process, which in turn remarkably affect the properties of these materials.

StJohn and Hogan<sup>[6]</sup> classified peritectic alloys into three types (A, B and C) according to the compositional range of the peritectic phase. In type A and B, the peritectic phase composition range is wide and the formation of microstructures has been extensively researched, such as alternating bands of primary phase and peritectic phase in Sr-Cd and Pb-Bi alloys<sup>[7, 8]</sup> at high  $G/v$  values ( $G$  and  $v$  are the temperature gradient and growth rate, respectively), simultaneous growth microstructures in Ni-Al and Fe-Ni alloys<sup>[2, 9]</sup> at low growth rates. However, few studies have been investigated on

the formation of microstructures in type C, for the reason that the peritectic phase compositional range is small and the peritectic phase is often an intermetallic or stoichiometric compound, as shown in Cu-Sn, Nd-Fe-B and Y-Ba-Cu-O peritectic systems. It is reported that the growth mechanism of the peritectic phase in YBCO<sup>[10]</sup>, unlike that of type A and B, in which the peritectic 123 phase has been observed to grow and solidify through the disappearance of primary 211 phases dissolved into the liquid. Due to the growth anisotropy of intermetallic compounds, it is less understood that the solidification behaviors of peritectic alloys in type C, especially in the field of microstructure formation and the growth mechanisms of the peritectic phase.

In this paper, directionally solidified Cu-75%Sn peritectic alloy is carried out to study the feature of microstructure formation and the growth mechanism of peritectic  $\eta$  phase at different growth rates in directional solidification.

## 2 EXPERIMENTAL

Cu-Sn peritectic alloy was prepared from the pure Sn (99.9%) and Cu (99.99%). The charge

① **Foundation item:** Projects(50395102; 50401014) supported by the National Nature Science Foundation of China; DPOP Project supported by the NWPU

**Received date:** 2004-12-14; **Accepted date:** 2005-01-18

**Correspondence:** LI Shuang-ming, Associate Professor; Tel: +86-29-88493264; E-mail: lsm@nwpu.edu.cn

was melted by a resistance heating furnace in an alumina crucible. The composition of the ingot analyzed by ICP was 75% Sn and 25% Cu (mass fraction, %). The machined sample was put in a high-purity alumina tube with 115 mm in length and 7.1 mm in diameter. It was remelted by an induction coil in a directional solidification apparatus. Directionally solidified specimens were cut down and metallographically polished in longitudinal and transverse sections, respectively. Metallographic specimens were etched by a solution of 5 g  $\text{FeCl}_3$  + 10 mL  $\text{HCl}$  + 100 mL  $\text{H}_2\text{O}$ . An Olympus PM-T3 microscope was employed to investigate the solidified specimen microstructures and Leica Quantimet 500 Image Processing and Analysis System was used to measure the primary dendritic arm spacing and sizes of the primary  $\epsilon$  phase and peritectic  $\eta$  phase.

### 3 RESULTS AND DISCUSSION

#### 3.1 Directionally solidified microstructures

In an equilibrium solidification process,  $\epsilon$  phase is firstly precipitated from the liquid in Cu-75% Sn peritectic alloy, and then peritectic  $\eta$  phase

is produced by the peritectic reaction at the peritectic temperature  $T_p$ , 415 °C ( $\epsilon + L \xrightarrow{\text{415 } \text{C}} \eta$ ). The remained liquid solidifies to the eutectic ( $\eta + \text{Sn}$ ) by the eutectic reaction at 227 °C ( $L \xrightarrow{\text{227 } \text{C}} \eta + \text{Sn}$ ). Thus, the equilibrium microstructure of Cu-75% Sn peritectic alloy only consists of peritectic  $\eta$  phase, the eutectic without any primary  $\epsilon$  phases.

Fig. 1 shows the directionally solidified microstructures of Cu-75% Sn peritectic alloy in longitudinal section grown at 1, 10, 100 and 300  $\mu\text{m/s}$ , respectively. It indicates that the gray-like phase is the primary  $\epsilon$  phase coated by the white peritectic  $\eta$  phase and the black phase between them is the eutectics by the composition analysis in different phases, which agrees with peritectic reaction resulting in the primary phase enveloped by the peritectic phase. Fig. 2 illustrates the solidification microstructures of Cu-75% Sn peritectic alloy in transverse section grown at 1, 3, 10, 50, 100 and 300  $\mu\text{m/s}$ , respectively. In Figs. 1(a) and 2(a), primary  $\epsilon$  phases disperse in the matrix of  $\eta$  phases, because  $\eta$  phases have enough time to grow at very slow growth rate of 1  $\mu\text{m/s}$  and finally, they can connect together. At growth rate ranging from 1 to 300  $\mu\text{m/s}$ , the directionally solidified micro-

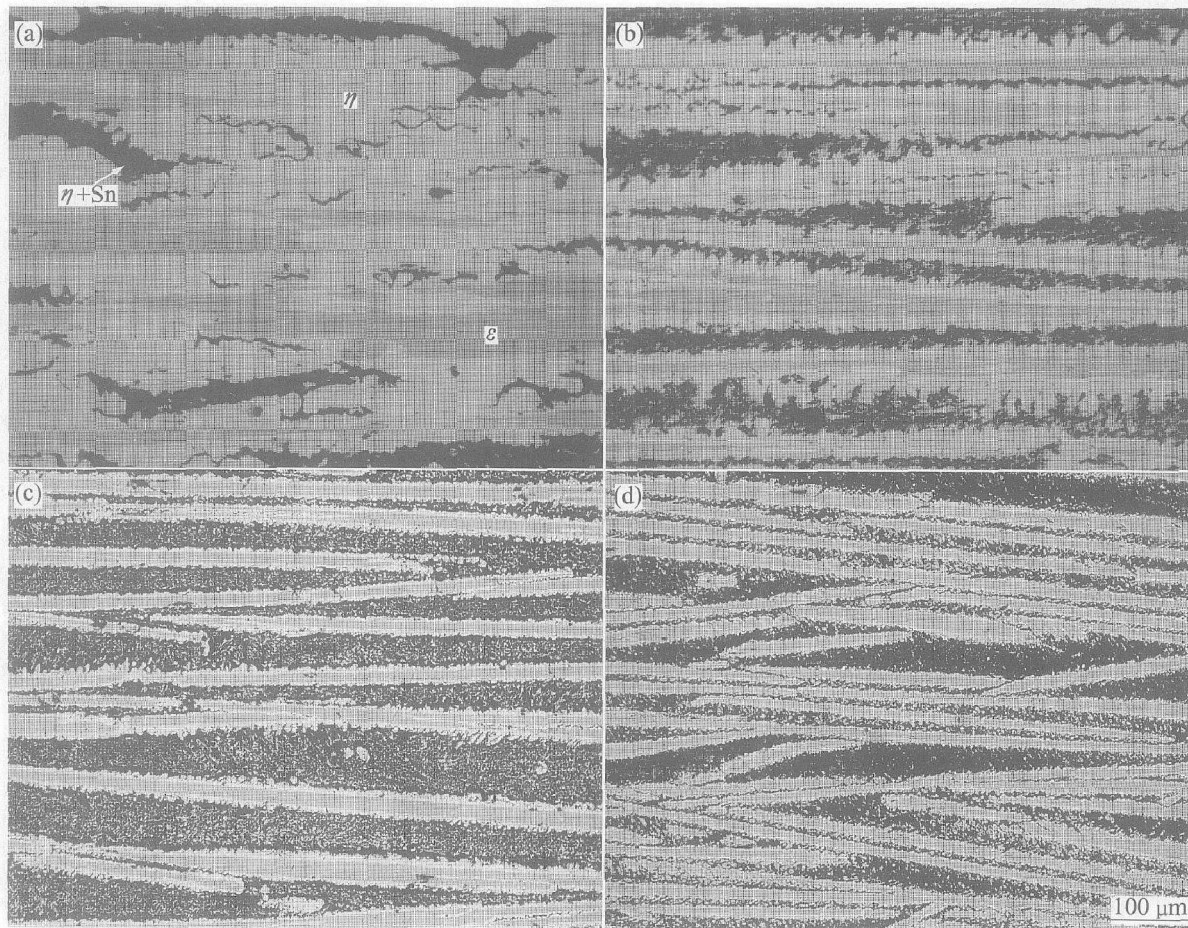


**Fig. 1** Directionally solidified microstructures of Cu-75% Sn peritectic alloy in longitudinal section at various growth rates  
 (a)  $v = 1 \mu\text{m/s}$ ; (b)  $v = 10 \mu\text{m/s}$ ; (c)  $v = 100 \mu\text{m/s}$ ; (d)  $v = 300 \mu\text{m/s}$

structure consists of the primary  $\epsilon$  phase and the peritectic  $\eta$  phase and the eutectic, which is different from the equilibrium microstructure. Plate-like microstructure containing  $\epsilon$  and  $\eta$  phases shown in Figs. 1 and 2 has been refined not only by decreasing growth time, but also by increasing nucleation quantities of  $\epsilon$  phases due to the larger undercooling in undercooled melt at higher growth rate.

### 3.2 Peritectic $\eta$ phase growth

After peritectic reaction, peritectic phase will envelope the primary phase preventing the direct contact between the primary phase and the liquid. At this time, peritectic reaction will not continue and peritectic phase growth will depend on other growth mechanisms.

As shown in Figs. 1 and 2, the interface morphologies of  $\epsilon$  phase and  $\eta$  phase are uneven, for example, peritectic  $\eta$  interface morphology con-

necting with the liquid is cellular. This means that peritectic  $\eta$  phase grows directly not only to the primary  $\epsilon$  phase by depleting of  $\epsilon$  phase controlled by the solid phase diffusion, but also to the undercooled melt, if not, the faceted primary  $\epsilon$  and peritectic  $\eta$  phase will grow with smooth surfaces. The first process for the peritectic  $\eta$  phase growth is called peritectic transformation and the second process is the direct solidification. Accordingly, the growth mechanism of peritectic  $\eta$  phases involved in Figs. 1 and 2 is very clear to distinguish as peritectic transformation and direct solidification from the undercooled melt.

In addition, peritectic  $\eta$  phase are coated by primary  $\eta$  phase shown in the circles of Fig. 2. It is different from the peritectic reaction in which the primary  $\epsilon$  phase is enveloped by the peritectic  $\eta$  phase. This phenomenon opposition to the results of peritectic reaction may be contributed as the fol-

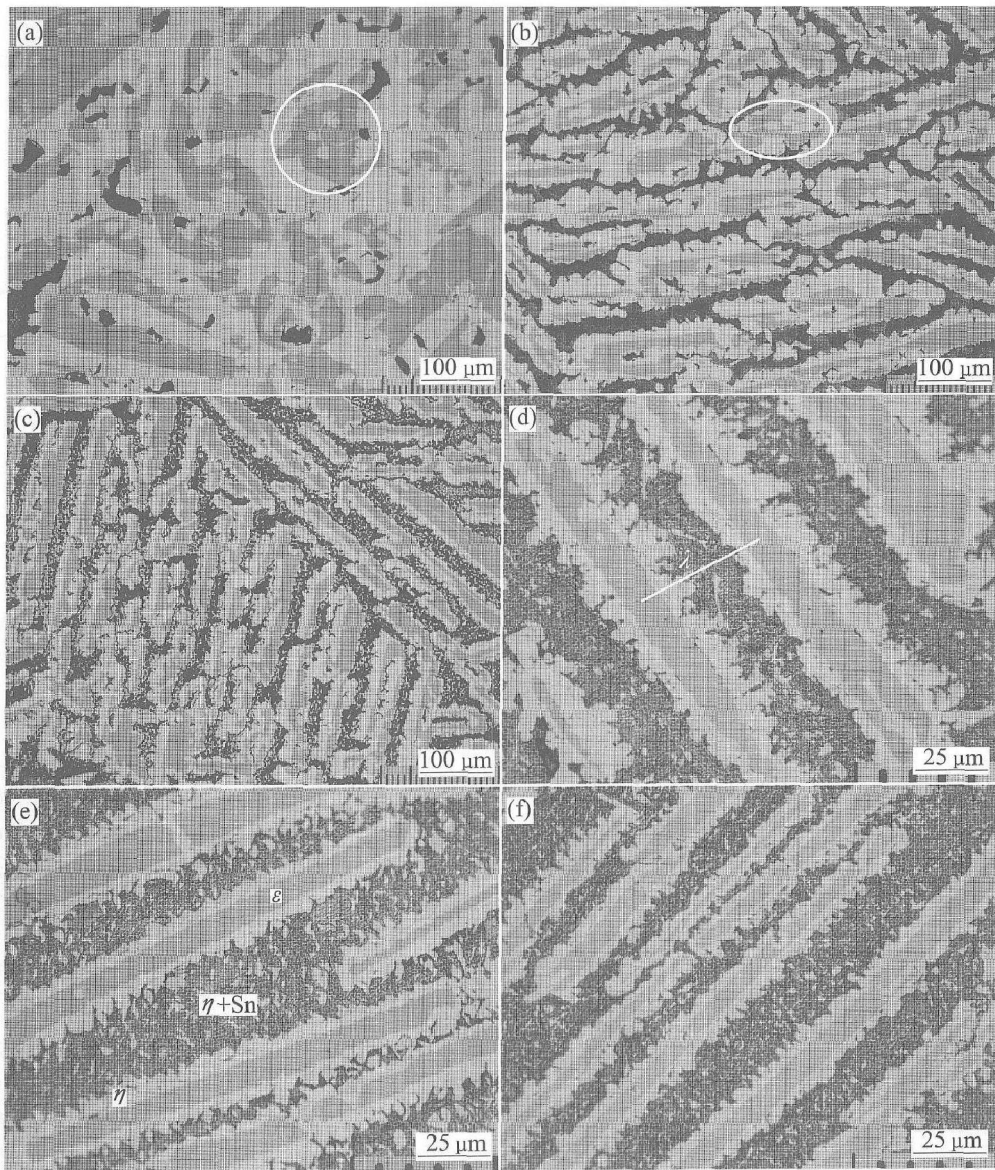


**Fig. 2** Directionally solidified microstructures of Cu-75%Sn alloy in transverse section at various growth rates

(a)  $v = 1 \mu\text{m/s}$ ; (b)  $v = 3 \mu\text{m/s}$ ; (c)  $v = 10 \mu\text{m/s}$ ; (d)  $v = 50 \mu\text{m/s}$ ; (e)  $v = 100 \mu\text{m/s}$ ; (f)  $v = 300 \mu\text{m/s}$

lowing factors: one is that primary  $\epsilon$  phase is a metastable phase at the temperature below  $T_p$ , and peritectic  $\eta$  phase is a stable phase. If kinetic conditions are suitable for the nucleation and growth of peritectic  $\eta$  phases in primary  $\epsilon$  phases, primary  $\epsilon$  phases will be transformed to peritectic  $\eta$  phases. Another reason is that the peritectic  $\eta$  phase grows in different directions. If the tip of the peritectic  $\eta$  phase grows into the primary  $\epsilon$  phase, the primary  $\epsilon$  phase will be transformed to the peritectic  $\eta$  phase resulting in the peritectic  $\eta$  phase surrounded by the primary  $\epsilon$  phase as seen in Fig. 2. The last factor is that  $\eta$  phase may grow between two primary  $\epsilon$  phases, thus in longitudinal and transverse sections,  $\eta$  phase enveloped by  $\epsilon$  phases will appear.

### 3.3 Sizes of $\epsilon$ phase and $\eta$ phase as well as primary dendritic arm spacing

There is no suitable solidification model used to calculate the size and quantity of primary phase in peritectic system, thus, the single-phase alloy solidification theory or eutectic solidification theory model are introduced to calculate sizes of different phases in peritectic system. According to Kurz-Fisher model<sup>[11]</sup>, one can obtain the dendritic tip radius given by

$$r = 2\pi \left[ \frac{D_L \Gamma_\epsilon}{v k_\epsilon \Delta T_\epsilon} \right]^{0.5} = A v^{-0.5} \quad (1)$$

where  $r$  is the dendritic tip radius,  $D_L$  is the diffusion coefficient in the liquid,  $\Gamma_\epsilon$  is the Gibbs-Thomson coefficient,  $k_\epsilon$  is the equilibrium distribution coefficient and  $\Delta T_\epsilon$  is  $\epsilon$  crystallization interval from its liquidus line temperature ( $T_L$ ) to the peritectic reaction temperature ( $T_p$ ). One can calculate the value of  $A$  in Eqn. (1) by the thermophysical parameters listed in Table 1.

**Table 1** Thermophysical parameters of Cu-75% Sn peritectic alloy<sup>[12, 13]</sup>

$T_L$ /K	$T_p$ /K	$T_e$ /K	$\Gamma_\epsilon$ /(m · K)	$D_L$ /(m <sup>2</sup> · s <sup>-1</sup> )	$k_\epsilon$
840	688	500	$5 \times 10^{-7}$	$5 \times 10^{-9}$	0.51

In the peritectic transformation process, the width of  $\epsilon$  transformed to  $\eta$  as function of time conforms the square root theory<sup>[14]</sup>, which can be written as

$$x = B t^{0.5} = B (\Delta T_\eta)^{0.5} (Gv)^{-0.5} \quad (2)$$

where  $x$  is the transformed width of  $\epsilon$  phase,  $t$  is time for growth of  $\eta$  phase,  $B$  is the parameter related to the alloy composition,  $G$  is the temperature gradient measured in the experiment as 200 K/cm, and  $\Delta T_\eta$  is the temperature interval for growth of  $\eta$  from the peritectic reaction temperature to the eutectic reaction temperature ( $T_e$ ). For Cu-75% Sn alloy, the value of  $B$  is assumed as  $10^{-7}$  m/s<sup>-0.5</sup> according to its peritectic  $\eta$  phase composition range<sup>[13]</sup>,

and then the width ( $W$ ) can be obtained as

$$W = 2(r - x) = 2(A - B \Delta T_\eta^{0.5} G^{-0.5}) v^{-0.5} \quad (3)$$

Measured widths of  $\epsilon$  and the whole plate-like microstructure containing  $\epsilon$  and  $\eta$  in the experiment and the theoretical results calculated using Eqn. (1) and Eqn. (3) are given in Fig. 3. It shows that with increasing growth rate, the width of the whole plate-like microstructure ( $W$ ) decreases and the regressed data fit with  $Wv^{0.27} = 117 \mu\text{m}^{1.27} \cdot \text{s}^{-0.27}$ . The difference between the size of the whole plate-like microstructure and that of the single phase calculated by Eqn. (1) increases at higher growth rates as shown in Fig. 3, because the solute dissipating from the primary  $\epsilon$  phase benefits growth of the peritectic  $\eta$  phase. Moreover, the measured data larger than the calculated results originates from the plate-like microstructure dendritic tip radius is not simply treated as the hemisphere morphology illustrated in Eqn. (1) and unknown exactly physical parameters in Cu-75% Sn alloy are also important factors leading to the deviation results.

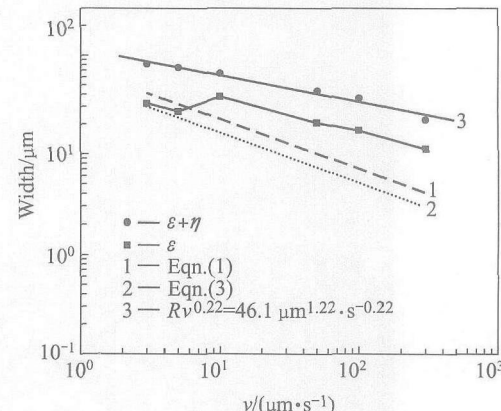


**Fig. 3**  $\epsilon$  phase and whole plate-like microstructure as function of growth rates

In Fig. 3, it is seen that at low growth rate varying from 5 to 10  $\mu\text{m}/\text{s}$ , the width of  $\epsilon$  phase increases, which is opposite to the results calculated by Eqns. (1) and (3). The main reason is that at lower growth rate, the primary  $\epsilon$  phase will grow in larger size, but it will also be depleted by the peritectic transformation contributing to the growth of  $\eta$  phase, resulting in that the width of  $\epsilon$  phase at the growth rate of 5  $\mu\text{m}/\text{s}$  is less than that at the growth rate of 10  $\mu\text{m}/\text{s}$  owing to increasing the transformation time. At higher growth rates, the deviation between the size of  $\epsilon$  phase and the whole plate-like microstructure enlarges resulting from rapid growth of  $\eta$  phase at higher undercooled melt.

Primary dendritic arm spacing of Cu-75% Sn alloy is also the primary  $\epsilon$  dendritic arm spacing as shown in Fig. 2(d), which can be calculated by

single-phase solidification model. Fig. 4 shows primary  $\epsilon$  dendritic arm spacing ( $\lambda$ ) measured by the experiment and calculated by BH model<sup>[15]</sup>, KF model<sup>[11]</sup> and Hunt-Lu numerical model<sup>[16]</sup>, indicating that the regressed experimental value of  $\lambda^{0.208}$  is constant as  $153.8 \mu\text{m}^{1.208} \cdot \text{s}^{-0.208}$  at growth rate ranging from 3 to 300  $\mu\text{m}/\text{s}$ . The regressed exponent value of the growth rate is close to those of BH model and KF model, but it is different from that of Hunt-Lu numerical mode as shown in Fig. 4. The value difference between experimental data and calculated results may be contributed to various solidification behaviors between peritectic system and single-phase system. The single-phase theoretical model of primary dendritic arm spacing is derived from the non-faceted phase growth and it is not well reasonable for calculating the primary dendritic arm spacing of Cu-75%Sn peritectic alloy, because primary  $\epsilon$  phase and peritectic  $\eta$  phase grow as faceted phases<sup>[14]</sup>. Another factor is the unknown exact thermophysical property parameters of Cu-75%Sn alloy. These analysis results illustrate that a new theoretical model should be developed to further investigate the dendritic arm spacing in directional solidification of peritectic alloys.

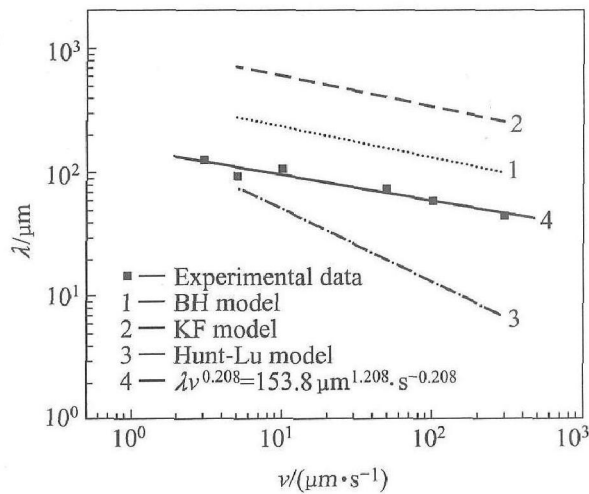


**Fig. 4** Primary dendritic arm spacing of Cu-75 %Sn alloy as function of growth rate

#### 4 CONCLUSIONS

1) Peritectic  $\eta$  phase can grow by the peritectic transformation and direct solidification from the liquid and directionally solidified plate-like microstructures in Cu-75%Sn peritectic alloy are refined as the growth rate increases from 1 to 300  $\mu\text{m}/\text{s}$ .

2) At low growth rate varying from 5 to 10  $\mu\text{m}/\text{s}$ , the width of  $\epsilon$  phase increases due to the peritectic transformation. At higher growth rate, the deviation between the widths of primary  $\epsilon$  phase and the whole plate-like microstructure increases originating from direct solidification of  $\eta$

phase from the undercooled melt.

3) The regressed data show that the relationship between the width of the whole plate-like microstructure ( $W$ ) and the growth rate ( $v$ ) satisfies  $W v^{0.27} = 117 \mu\text{m}^{1.27} \cdot \text{s}^{-0.27}$  and the primary dendritic arm spacing ( $\lambda$ ) with growth rate has a relation of  $\lambda^{0.208} = 153.8 \mu\text{m}^{1.208} \cdot \text{s}^{-0.208}$  as the growth rate increases from 3 to 300  $\mu\text{m}/\text{s}$ .

#### REFERENCES

- [1] Johnson D R, Inui H, Yamaguchi M. Crystal growth of TiAl alloys [J]. *Intermetallics*, 1998, 6: 647 - 652.
- [2] Lee J H, Verhoeven J D. Peritectic formation in the Ni-Al system [J]. *J Cryst Growth*, 1994, 144: 353 - 366.
- [3] Loser W, Herlach D M. Theoretical treatment of solidification of undercooled Fe-Cr-Ni melts [J]. *Met Trans*, 1992, 23A(5): 1585 - 1591.
- [4] Knoch K G, Reinsch B, Petzow G Z. NdFeB-Its region of primary solidification [J]. *Z Metallkd*, 1994, 85(5): 350 - 353.
- [5] Kerr H W, Kurz W. Solidification of peritectic alloys [J]. *Inter Mater Rev*, 1996, 41(4): 129 - 164.
- [6] StJohn D H, Hogan L M. A simple prediction of the rate of the peritectic transformation [J]. *Acta Metall*, 1987, 35: 171 - 174.
- [7] Brody H D, David S A. Controlled solidification of peritectic alloys [A]. *Solidification and Casting of Metals* [C]. London: The Metals Society, 1979. 144 - 150.
- [8] Trivedi R. Theory of layered microstructure formation in peritectic systems [J]. *Met Mater Trans*, 1995, 26A(6): 1583 - 1590.
- [9] Hunziker O, Vandyoussefi M, Kurz W. Phase and microstructure selection in peritectic alloys close to the limit of constitutional undercooling [J]. *Acta Mater*, 1998, 46(18): 6325 - 6336.
- [10] Chow J C L, Lettow J S, Waidl D A, et al. SmBa<sub>2</sub>Cu<sub>3</sub>O<sub>6.5</sub> seed fabrication for seeded peritectic solidification of YBa<sub>2</sub>Cu<sub>3</sub>O<sub>7-8</sub> [J]. *J Mater Sci*, 1998, 33(1): 133 - 137.
- [11] Kurz W, Fisher D J. *Fundamentals of Solidification* (4th ed) [M]. Switzerland: Trans Tech Pub, 1998. 63 - 89.
- [12] Fredriksson H, Nylen T. Mechanism of peritectic reactions and transformations [J]. *Met Sci*, 1982, 16 (6): 283 - 294.
- [13] Saunders N, Miodownik A P. *Phase Diagrams of Binary Copper alloys* [M]. USA: ASM International, 1994. 412.
- [14] Ha H P, Hunt J D. A numerical and experimental study of the rate of transformation in three directionally grown peritectic systems [J]. *Metall Mater Trans A*, 2000, 31A(1): 29 - 34.
- [15] Burden M H, Hunt J D. Cellular and dendritic growth I [J]. *J Cryst Growth*, 1974, 22: 99 - 108.
- [16] Hunt J D, Lu Su-zu. Numerical modeling of cellular/dendritic array growth: spacing structure prediction [J]. *Metall Mater Trans A*, 1996, A27(3): 611 - 623.

(Edited by LONG Huai-zhong)